ferent mobilities at different time scales, and a certain motion at a specific time scale may be responsible for expressing their biological functions.

The internal motions detected by the $R_{1\rho}$ measurements for the B- and Z-d$(CG)_3$ in 2 M $NaClO_4$ solution are in the time range of $1/\omega_1$. The $R_{1\rho}$ measurements reveal the important features of the internal motions of these molecules. Both the B- and Z-d$(CG)_3$ have exchange contributions, $R_{1\rho(ex)}$, indicating that both molecules have the internal motions in this time range. However, the magnitude of $R_{1\rho(ex)}$ for the B- and Z-d$(CG)_3$ is markedly different (Table III). $R_{1\rho(ex)}$ for the Z-d$(CG)_3$ is 2-3 times larger than that for the B-d$(CG)_3$.

The larger exchange contribution, $R_{1\rho(ex)}$, to the overall relaxation rates, $R_{1\rho(obsd)}$, of the Z-d$(CG)_3$ may arise from large chemical shift differences between conformational states. An alternative explanation is the larger amount of lower frequency components in the Z-d$(CG)_3$. Preliminary results demonstrate that the exchange lifetimes are in the range of 10-20 μs for the B- and Z-d$(CG)_3$. $R_{1\rho}$ can be measured at different ω_1 fields, and the analysis of the ω_1 dependence of $R_{1\rho}$ will provide information of both the exchange lifetimes and the chemical shift differences between sites independently. The chemical shift differences are considered to correlate with the magnitude of the amplitudes of the internal motions.[19] Further work along this line is in progress.

Acknowledgment. This research was supported by the Research Corp. and the American Chemical Society, Illinois Division, Grant 87-30. We wish to thank Drs. K. D. Kopple and J. Longworth for inspiring discussion. We thank J. Bernhardt for many helpful suggestions.

Ultrafast Ligand Rebinding to Protoheme and Heme Octapeptide at Low Temperature

Jay C. Postlewaite, Jeffrey B. Miers, and Dana D. Dlott*

Contribution from the School of Chemical Sciences, University of Illinois at Urbana Champaign, 505 South Mathews Avenue, Urbana, Illinois 61801. *Received May 2, 1988*

Abstract: Ultrafast flash photolysis is used to investigate the rebinding of carbon monoxide to protoheme (PH) and heme octapeptide (HO) in a glycerol-water glass at 100 K. Kinetic decay data are obtained at several probing wavelengths in the Soret bands. Previous work [Hill, J. R., et al. *Springer Ser. Chem. Phys.* **1986**, *46*, 433] had shown the existence of two distinct ligand rebinding processes. The first, denoted process I*, is exponential in time, with a rate of $\approx 3 \times 10^{10}$ s^{-1}. Process I* involves non-Arrhenius rebinding, as evidenced by a roughly linear dependence of the rate constant on temperature. The second, denoted process I, involves nonexponential rebinding which does obey the Arrhenius expression for a system with distributed activation barriers. Kinetic measurements performed at the isosbestic point between carboxy heme (denoted Fe-L) and deoxy heme (denoted Fe + L) demonstrate the existence of two short-lived intermediates (denoted Fe^1--L and Fe*--L). Multiple-flash experiments at 15 K show that these species cannot be easily interconverted, implying they exist as two distinct, inhomogeneous sets of reacting molecules. One reacting subensemble consists of Fe-L species which, upon photolysis, relax at a rate of $\approx 10^{12}$ s^{-1} into Fe + L and then rebind ligands via process I. The other consists of molecules which are unable to relax into Fe + L states, and which rebind ligands via process I*. The difference between the two subensembles is attributed to solvent interactions which constrain the geometry of some molecules to inhibit the relaxation process. The rebinding parameters of PH and HO are compared at 100 K. The HO differs from PH by the addition of a basket handle peptide chain which donates a proximal histidine. HO relaxes faster (1 ps) after deligation than does PH (1.5 ps). Process I* rebinding to unrelaxed hemes has nearly the same rate in PH and HO. This observation is consistent with a picture of ligand rebinding to planar, unrelaxed hemes which differ only in proximal substitution. Process I is much slower in HO, probably because proximal tension exerted by the peptide chain on the relaxed heme increases the activation barrier.

The rebinding of photodissociated neutral ligands to heme[1-3] has received considerable attention because heme derivatives have important catalytic properties and play a central role in enzyme biochemistry. In this work we report ultrafast, multispectral kinetic data on rebinding of carbon monoxide to iron(II) protoheme (PH) and heme octapeptide (HO) at low temperature (T = 100 K) in a solvent glass (glycerol-water 75:25). In these low-temperature systems, photolyzed ligands are confined in a glassy solvent cage surrounding each heme. Geminate rebinding to Fe can be studied without the complications induced by migration through a protein matrix or diffusion through the solvent.[4-6]

The processes we study can be divided into three stages. In the first stage, photodissociation, every heme is bound to a ligand, carbon monoxide (CO), and is denoted as the Fe-L state. The Fe-L complex is nearly planar, with low spin, $S = 0$.[3,5] Upon photoexcitation, the ligand moves away from Fe along a repulsive potential surface. The short-lived intermediate formed by the photolysis process will be denoted Fe--L. The spin state(s) of such Fe--L species are unknown at this time. The second stage involves the relaxation of this intermediate into the stable deligated heme, denoted Fe + L. The Fe + L species is characterized by a domed heme with high spin, $S = 2$.[3,5] Finally, the third stage involves ligand rebinding which transforms Fe + L into Fe-L molecules.

Heme octapeptide is prepared by enzymatic digestion of cytochrome c,[7] and it differs from PH by the presence of a "basket

* Author to whom correspondence should be addressed.

(1) DeBrunner, P. G.; Frauenfelder, H. *Annu. Rev. Phys. Chem.* **1982**, *33*, 283.
(2) Frauenfelder, H.; Parak, F.; Young, R. D. *Annu. Rev. Biophys. Biophys. Chem.* **1988**, in press.
(3) Antonini, E.; Brunori, M. *Hemoglobin and Myoglobin in Their Reactions with Ligands*; North Holland: Amsterdam, 1971.
(4) Austin, R. H.; Beeson, K. W.; Eisenstein, L.; Frauenfelder, H.; Gunsalus, I. C. *Biochemistry* **1976**, *14*, 5355.
(5) Alberding, N.; Austin, R. H.; Chan, S. S.; Eisenstein, L.; Frauenfelder, H.; Gunsalus, I. C.; Nordlund, T. M. *J. Chem. Phys.* **1976**, *65*, 4701.
(6) Hill, J. R.; Cote, M. J.; Dlott, D. D.; Kauffman, J. F.; McDonald, J. D.; Steinbach, P. J.; Berendzen, J. R.; Frauenfelder, H. *Springer Ser. Chem. Phys.* **1986**, *46*, 433.
(7) Harbury, H. A.; Loach, P. A. *J. Biol. Chem.* **1960**, *235*, 3640.

0002-7863/89/1511-1248$01.50/0

handle" peptide chain whose proximal histidine binds to Fe and mimics the hemeprotein structure. Thus comparison of these two compounds is expected to yield interesting information about the effect of this linkage on the relaxation and ligand rebinding processes. Such interactions are generally described by the term "proximal tension".[8] The spectra of the Fe–L and Fe + L species of HO[9] also indicate low-spin and high-spin states, respectively.

Carbon monoxide rebinding to PH and HO has been previously studied over a wide temperature range by Frauenfelder and colleagues[5,9] and Marden et al.[10] These studies did not have sufficient time resolution to observe heme relaxation and the ultrafast component of ligand rebinding. Many synthetic model heme compounds have been the subject of ambient-temperature ultrafast studies,[11,12] and the rebinding of CO and other ligands to various model compounds has been observed by Traylor and colleagues.[13,14] Martin et al.[15] also studied PH–CO at ambient temperature with subpicosecond resolution. However, the ultrafast work was not extended to the low-temperature regime. Conversely, low-temperature measurements have been conducted by Tetreau et al.[16] on a series of model heme compounds, but without ultrafast time resolution.

Previously Hill et al.[6] reported preliminary ultrafast data (t_r = 2 ps) on PH–CO kinetics in the 50–300 K range. The molecules were photolyzed and probed at 565 nm. At 300 K, they observed two rebinding processes, nonexponential geminate rebinding on the ≈100-ps time scale (process I), and slow, diffusion-limited exponential rebinding on the ≈100-μs time scale (solvent process). The work of Hill et al. appears to be the first observation of ambient temperature geminate CO rebinding to protoheme. Previous studies had accessed time scales which were either too long[5,9] or too short[15] to observe the ≈100-ps nonexponential recombination. As the temperature was lowered below T_g of the glassy matrix, the solvent process vanished, and process I remained nonexponential but slowed considerably. An exponential rebinding process, process I*, with a time constant of tens of picoseconds, was observed. Process I* does not obey the Arrhenius law.[6,17] Rather the rate of process I* is a nearly *linear* function of temperature[6] in the 80–180 K range.

We have now constructed a kinetic spectrometer which permits us to probe at any λ in the Soret (ca. 380–460 nm) region, and used it to investigate PH and HO rebinding. The multispectral capability is an important improvement because it allows us to partially isolate the dynamics of Fe–L and Fe + L via spectral selection, and to totally isolate the dynamics of short-lived Fe··L transients by probing near the isosbestic point[17,18] of Fe–L and Fe + L. We have developed a kinetic model which accurately replicates our data and provides a convincing mechanism for process I*, namely that it involves ultrafast rebinding to heme molecules which do not relax from the Fe··L state to the Fe + L state. The parameters obtained from this model for PH and HO permit an interesting comparison of these substances at 100 K. Heme relaxation is faster and slightly more complete in HO compared to PH, a consequence of the proximal linkage in HO. Process I* is nearly identical in the two materials, as expected for rebinding to unrelaxed, planar hemes which differ only in proximal configuration. Process I is considerably slower in HO than in PH, again a consequence of the proximal linkage.

Experimental Methods

Protoheme (hemin) and heme octapeptide were obtained from Sigma Chemical Co. and used without further purification. The method of sample preparation has been previously described by Chan.[9] Briefly, the hemin is dissolved in a basic (NaOH) solution of glycerol–water (75:25) at pH 10, saturated with CO gas, and reduced with sodium dithionite. The HO is dissolved in Tris buffer, pH 7, mixed in glycerol with the same proportions as protoheme, saturated with CO, and reduced. The heme concentration was ≈5×10^{-4} M. These methods of preparation result in well-characterized samples with a minimum of aggregation.[9]

The samples were held between sapphire windows with a Teflon spacer, and placed in a closed-cycle helium refrigerator. The temperature was measured with a calibrated Si diode and controlled to ±0.2 K with a digital, proportional controller. The spacer thickness was adjusted in the vicinity of 1 mm to obtain an optical density at the absorption peak of about unity.

The laser photolysis apparatus consisted of a rhodamine 6G dye laser synchronously pumped by a frequency-doubled, mode-locked Nd:YAG laser.[19] With a two-plate birefringent filter, the output pulse was nearly transform limited, making the usual assumption of a sech^2 pulse shape.[20] The full width at half-maximum of the autocorrelation function was 3.5 ± 0.5 ps (the errors indicate day-to-day pulse width drift rather than inaccuracy in measurements on a given day), giving a pulse width of 2.0 ps.[20] The dye laser was amplified at variable pulse repetition frequency (PRF) between 0 and 1000 Hz using the synchronous, 85-ps, 1-mJ output of a previously described Nd:YAG regenerative amplifier.[19] The output pulse was not detectably broadened by the amplification, and its energy was typically 40 μJ at 570 nm.

About one-half of the laser pulse is used to produce a white light continuum pulse[20,21] in a 10-cm cell of water. The blue portion of this pulse was isolated with a dichroic mirror. The remaining 570-nm photolysis pulse was focused to a Gaussian beam radius of 100 μm in the sample. The broad-band blue probe pulse was focused to a slightly smaller spot size ($\omega \approx 75$ μm) by the same lens by virtue of its shorter wavelength. The probe pulse interrogated the sample and was then focused onto the entrance slit of a double 0.5-m monochromator with dual 1800 l/mm gratings. The monochromator was used to isolate a particular spectral portion of the continuum pulse. The data presented in this work were obtained with a bandpass of 0.1–0.2 nm although increasing the bandpass to 1 nm had no discernible effect on the kinetic decays. The probe pulse was detected by a low gain photomultiplier (RCA 1P28A), and the signal was fed into a lock-in amplifier, signal averager, and computer.

Usually one sends the photolysis pulse into the sample with fixed delay while mechanically scanning the delay of the probe pulse. We found it advantageous to reverse the procedure by scanning the photolysis delay in the reverse direction. When mechanically delaying the probe, special care must be taken to ensure that the probe pulse spatial profile does not change at several locations, namely, at the sample, at the entrance slit of the monochromator, at the exit slit, and on the surface of the photocathode. With a fixed probe and scanned photolysis pulse, the only constraint is that the photolysis pulse profile must remain constant at the sample. The delay line was repetitively swept at ≈0.2 Hz, and a few hundred decays were averaged for each data set. The averaged probe intensity before photolysis, $\tau < 0$, is called I_0. The intensity for $\tau > 0$ is called $I(\tau)$. Near the end of each delay scan, the probe pulse is electronically shuttered, and the average signal in this region, B, is a (nearly zero) baseline correction for photomultiplier dark current and scattered photolysis light. The computer was used to calculate $\Delta OD_\lambda(\tau)$, defined as

$$\Delta OD_\lambda(\tau) = -\log\left[\frac{I(\tau) - B}{I_0 - B}\right] \quad (1)$$

The photolysis pulse was tuned into the ^{1}Q origin (using the notation of

(8) Traylor, T. G. *Acc. Chem. Res.* **1981**, *14*, 102.
(9) Chan, S. Ph.D. Dissertation, University of Illinois, 1976.
(10) Marden, M. C.; Hazard, E. S., III; Gibson, Q. H. *Biochemistry* **1986**, *25*, 2786.
(11) Cornelius, P. A.; Steele, A. W.; Chernoff, D. A.; Hochstrasser, R. M. *Chem. Phys. Lett.* **1981**, *82*, 9. Liang, Y.; Negus, D. K.; Hochstrasser, R. M.; Grunner, M.; Dutton, P. L. *Chem. Phys. Lett.* **1981**, *84*, 236.
(12) Olson, J. S.; McKinnie, R. E.; Mims, M. P.; White, D. K. *J. Am. Chem. Soc.* **1983**, *105*, 1522. Kirmaier, C.; Holton, D. *Chem. Phys.* **1983**, *75*, 305. Dixon, D. W.; Kirmaier, C.; Holton, D. *J. Am. Chem. Soc.* **1985**, *107*, 808.
(13) Caldwell, K.; Noe, L. J.; Ciccone, J. D.; Traylor, T. G. *J. Am. Chem. Soc.* **1986**, *108*, 6150.
(14) Hutchinson, J. A.; Traylor, T. G.; Noe, L. J. *J. Am. Chem. Soc.* **1982**, *104*, 3221. Traylor, T. G.; Magde, D.; Taube, D.; Jongeward, K. *J. Am. Chem. Soc.* **1987**, *109*, 5865.
(15) Martin, J. L.; Migus, A.; Poyart, C.; Lecarpentier, Y.; Astier, R.; Antonetti, A. *Proc. Natl. Acad. Sci. U.S.A.* **1983**, *80*, 173.
(16) Tetreau, C.; Lavalette, D.; Momenteau, M.; Lhoste, J.-M. *Proc. Natl. Acad. Sci. U.S.A.* **1987**, *84*, 2267.
(17) Doster, W.; Bowne, S. F.; Frauenfelder, H.; Reinisch, L.; Shyamsunder, E. *J. Mol. Biol.* **1987**, *194*, 299.
(18) Martin, J. L.; Migus, A.; Poyart, C.; Lecarpentier, Y.; Antonetti, A.; Orszag, A. *Biochem. Biophys. Res. Commun.* **1982**, *107*, 803.
(19) Postlewaite, J. C.; Miers, J. B.; Reiner, C. C.; Dlott, D. D. *IEEE J. Quantum. Electron.* **1988**, *QE-24*, 411.
(20) Fleming, G. R. *Chemical Applications of Ultrafast Spectroscopy*; Oxford University Press: New York, 1986.
(21) Alfano, R. R.; Shapiro, S. *Chem. Phys. Lett.* **1972**, *8*, 631. Baldeck, P. L.; Ho, P. P.; Alfano, R. R. *Rev. Phys. Appl.* **1987**, *22*, 1677.

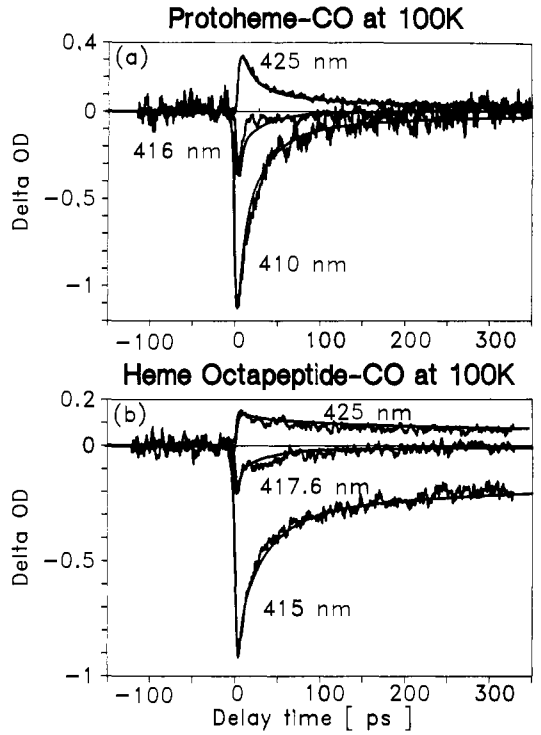

Figure 1. Kinetic data of the form $\Delta OD_\lambda(\tau)$ for (a) protoheme–CO (PH) and (b) heme octapeptide–CO (HO). The 425-nm data are taken near the peak of the relaxed Fe + L absorption, λ_{DL}; the 410- (PH) or 415-nm (HO) data are taken near the peak of the Fe–L absorption, λ_{CO}; and the 416- (PH) or 417.6-nm (HO) data are taken near the isosbestic point, λ_{IB}. The λ_{CO} data show a ≈30-ps exponential process, and a long, nonexponential tail. The λ_{DL} data show a delayed rise time relative to λ_{CO}, and the same nonexponential tail. The λ_{IB} data show the presence of *two* short-lived intermediates, one associated with the delayed rise time, and one associated with the ≈30-ps exponential decay. The smooth curves are a fit to the data using eq 10–13. The fitting parameters are given in Table I.

Chernoff et al.[22]) at ca. 570 nm, as this gives efficient photolysis with minimal sample heating and degradation. As the intensity of the photolysis pulse is increased, the photolysis process will eventually saturate. We carefully adjusted the intensity of this pulse to the minimum which will photolyze ≥90% of the ligated heme molecules. At this level, the observed decay function was *independent* of photolysis pulse energy, and the maximum ΔOD is nearly independent of pulse energy. The pulse energy necessary to enter this regime was on the order of 10 μJ, but depended somewhat on the sample OD. The decays we obtained were also independent of probe pulse intensity. The laser PRF was decreased until the observed decays became independent of PRF. This limit was reached at ca. 250 Hz at 100 K, and the 100 K data were obtained at a conservative PRF of 130 Hz.

Experimental Results

Heme Spectra. We will employ the notation that λ_{CO} denotes the Soret absorption maximum of the Fe–L species, λ_{DL} denotes the Soret absorption maximum of the equilibrium (deligated) Fe + L species, and λ_{IB} denotes the wavelength of the isosbestic point which lies roughly midway between λ_{CO} and λ_{DL}. For PH, $\lambda_{CO} \approx 410$ nm, $\lambda_{IB} \approx 416$ nm, and $\lambda_{DL} \approx 423$ nm.[9] For HO, $\lambda_{CO} \approx 415$ nm, $\lambda_{IB} \approx 418$ nm, and $\lambda_{DL} \approx 425$ nm.[9]

Kinetic Decays. Protoheme–CO and HO–CO were studied at a variety of probe wavelengths between 380 and 440 nm at $T = 100$ K, a temperature well below the solvent glass transition $T_g = 173$ K.[23] In Figure 1 we show kinetic decays, which have the functional form $\Delta OD_\lambda(\tau)$ for PH (Figure 1a) and HO (Figure 1b). The functional form of these decays was reproduced with several different samples. The displayed data were taken near λ_{CO}, λ_{IB}, and λ_{DL}. The smooth curves are the fit to a model discussed in the next section. When the carboxy heme samples were replaced by five-coordinate deoxy heme with no CO bound to Fe, no transient absorption changes could be detected by our apparatus.

The λ_{CO} data reflect *mostly* the photolysis and subsequent reappearance of Fe–L species, while the λ_{DL} data reflect *mostly* the appearance of subsequent disappearance of Fe + L species. The term "mostly" is invoked because the Fe–L and Fe + L Soret spectra are broad and overlapping.[9] Thus Fe–L has some absorbance at λ_{DL}, while Fe + L has some absorbance at λ_{CO}.

When three or more species with broad overlapping absorption spectra coexist, separating their individual kinetic behavior can be quite difficult. An important experimental technique to effect this separation involves *isosbestic probing*. Here we use the term isosbestic in a general sense: an isosbestic of two species, [A] and [B], is a point, λ_{IB}, where the extinction coefficients of [A] and [B] are equal. Consider a three-component system which at $\tau = 0$ is entirely composed of specie $[A(\tau = 0)] = A_0$. After photolysis, the system consists of $[A(\tau)]$, $[B(\tau)]$, and $[C(\tau)]$, where $[A] + [B] + [C] = A_0$ for all τ. Each species is characterized by its absorption spectrum, $\epsilon_{[i]}(\lambda)$, where ϵ is the decadic molar extinction coefficient. Measurements of the $\Delta OD_\lambda(\tau)$ subsequent to photolysis give

$$-\Delta OD_\lambda(\tau)/l = \{A_0 - [A(\tau)]\}\epsilon_{[A]}(\lambda) - [B(\tau)]\epsilon_{[B]}(\lambda) - [C(\tau)]\epsilon_{[C]}(\lambda) \quad (2)$$

where l is the optical path length. Equation 2 shows that, in general, all three species contribute to the kinetic decay obtained at λ. However, at the isosbestic point of [A] and [B], $\epsilon_{[A]}(\lambda_{IB}) = \epsilon_{[B]}(\lambda_{IB}) = \epsilon_0$, and

$$-\Delta OD_\lambda(\tau)/l = (\epsilon_0 - \epsilon_{[C]})[C(\tau)] \quad (3)$$

Equation 3 shows that at λ_{IB}, the contributions from [A] and [B] exactly cancel, and the observed kinetic decay yields the time-dependent behavior of [C]. In a three-component system, there may exist several such "isosbestic points" at which the contributions from two of the species exactly cancel. It would thus be highly desirable to probe each of these points and experimentally separate the kinetic behavior of each species. Doster et al.[17] used this technique in a study of time-dependent CO rebinding to horse radish peroxidase. At low temperature, two rebinding processes labeled process I (power-law nonexponential) and process I* (exponential) were observed. At arbitrary wavelengths, kinetic decays consisted of both components, but at two "isosbestic" locations, decays that were purely power law or purely exponential were observed.

Equation 3 also makes an interesting point concerning the *amplitude* of the kinetic decay obtained at λ_{IB}. Even if $\epsilon_{[C]}(\lambda_{IB})$ is exactly zero, the λ_{IB} decay still gives only the time-dependent behavior of [C], with the amplitude of the decay being proportional to ϵ_0, the extinction coefficient of [A] and [B] at λ_{IB}. In effect, the behavior of $[C(\tau)]$ is manifested through the time-dependent absence of $[A(\tau)] + [B(\tau)] \neq A_0$ to an extent determined by ϵ_0. This provides a convenient method to determine the kinetic behavior of species which are "invisible", that is, species which have no appreciable absorbance in the spectral region being probed.

Returning to Figure 1, the λ_{CO} data show an instantaneous [i.e., within instrument resolution of ≈1 ps] decrease in ΔOD. The recovery of the OD change consists of a fast ($\tau \approx 30$ ps), nearly exponential decay, and a smaller amplitude, slower transient which is nonexponential.

The λ_{DL} data show a delayed rise time relative to the λ_{CO} data. This delay is seen clearly in Figure 2. For this figure, we normalized the λ_{CO} (solid curve) and λ_{DL} (broken curve) data to the value of unity to facilitate comparison. The 570-nm laser pulse autocorrelation function is also shown (dotted curve). The experimental time resolution of our apparatus is somewhat faster than this function because the experiment employs one 570-nm laser pulse and the blue continuum pulse. As picosecond continuum pulses are known to be considerably shorter than their generating pulses,[21] the autocorrelation function is the *upper limit*

(22) Chernoff, D. A.; Hochstrasser, R. M.; Steele, A. W. *Proc. Natl. Acad. Sci. U.S.A.* **1980**, *77*, 5606.
(23) Birge, N. O.; Nage, S. R. *Phys. Rev. Lett.* **1985**, *54*, 2674. Jeong, Y. H.; Nage, S. R.; Bhattacharya, S. *Phys. Rev.* **1986**, *A34*, 602.

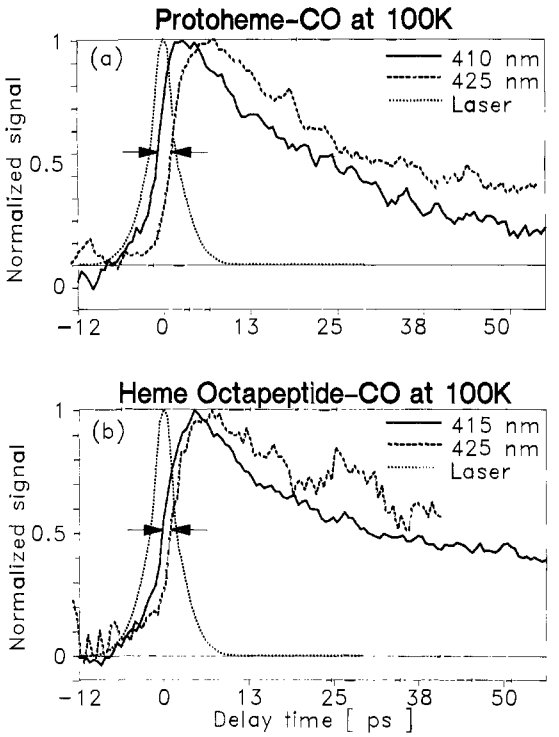

Figure 2. Expanded time view of λ_{CO} (solid line) and λ_{DL} (dashed line) data for PH and HO. The data are normalized to unity to facilitate comparison. The λ_{DL} data show a delayed rise relative to the λ_{CO} data, indicated by the pair of arrows. The laser apparatus autocorrelation function, an *upper limit* to the system time resolution, is indicated by the dotted line.

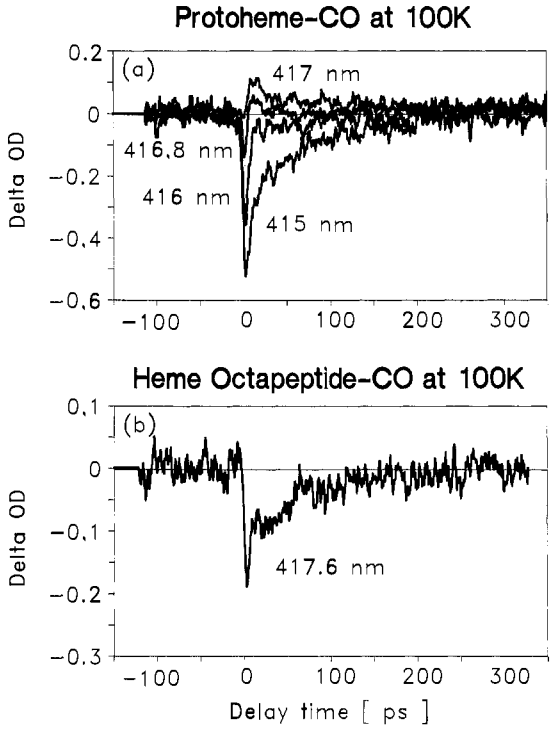

Figure 3. Kinetic data taken near the isosbestic point. The data show the presence of two intermediates, one which decays in a few picoseconds, and the other which decays in ≈30 ps.

to the instrument response for this experiment.

The λ_{DL} decay is shifted to longer time relative to the λ_{CO} decay for PH and HO. Before quantifying the shift, the effects of optical dispersion should be considered.[15] We carefully measured the dispersion in our system by correlating the 570-nm photolysis pulse with probes at either 570, 425, or 410 nm. The correlations were performed using background-free autocorrelation in a nonlinear KDP crystal and the saturation of laser dye solutions (e.g., LDS 722 from Exciton Corp.) which absorbed at the appropriate wavelengths. We found that the relative time delay of our apparatus, assuming the dispersion is linear in λ, was 74 (±3) fs/nm. This λ-dependent time delay has almost no broadening effect on the 2-ps, ≈1-nm bandwidth excitation pulse, but does produce a time delay differential of roughly 1 ps between the arrival of the λ_{CO} and λ_{DL} probe pulses.

To prepare Figure 2, we set the zero of time delay at the 50% point of the λ_{CO} data, because it is known from Petrich et al.[24] that bleaching of PH–CO occurs within 50 fs of excitation. We then shifted the λ_{DL} by 1.1 ps (PH) or 0.74 ps (HO) to compensate for dispersion. The resultant time shift, indicated by a pair of arrows, is 1.9 ps for PH and 1.2 ps for HO. We are thus observing a true delay in the formation of Fe + L relative to the disappearance of Fe–L species.

We can estimate the quantum yield, f, for photoproduction of the Fe + L species from Fe–L using the room-temperature extinction coefficients of Fe–L and Fe + L[9] at λ_{CO} and λ_{DL}. Given the observed decrease in ΔOD at λ_{CO} in Figure 1, a and b, we predict, for an assumed quantum yield $f = 1$, that the maximum ΔOD values at λ_{DL} should be 0.6 (PH) and 0.25 (HO). Instead, the observed values are 0.3 (PH) and 0.15 (HO), indicating that $f < 1$, but somewhat larger for HO relative to PH. A more detailed analysis of the quantum yield, which considers the effect of finite duration laser pulses, is performed in the Discussion.

Kinetic decays were obtained at 0.1-nm intervals, using a detection bandwidth of 0.1 nm, in the vicinity of $\lambda_{1B} \approx 417$ nm. A variety of transients, which were highly dependent on λ, were observed. Figure 3a shows the behavior of kinetic decays at several wavelengths in the vicinity of λ_{1B} for PH. To the blue of λ_{1B}, at 415 nm, $\Delta OD(\tau) \leq 0$ for all τ. A large contribution from the ≈30-ps exponential decay and the slow nonexponential decay is observed. At 416 nm, $\Delta OD(\tau) \leq 0$, and only a very fast (ca. 2 ps) process and a smaller amplitude tail can be observed. To the red of 416 nm (e.g., 416.8, 417 nm), the data show an initial drop in ΔOD, followed by a fast rise across the ΔOD = 0 line. Subsequently, ΔOD recovers via the nonexponential process.

From these data, we can surmise the properties of the transient difference spectra, $\Delta OD_\tau(\lambda)$ in the vicinity of λ_{1B}. For $\tau > 150$ ps, after all Fe--L species have decayed, the system has only two species remaining. The isosbestic, or zero crossing, will then occur exactly at $\lambda_{1B} \approx 416$ nm. For $\tau < 150$ ps, when three or four species are present, the instantaneous zero crossing occurs at different wavelengths, located to the blue of λ_{1B}. Put another way, the wavelength of the zero crossing occurs at different times. For example, Figure 3a shows that for PH, the zero crossing occurs at 416.8 nm at $\tau \approx 10$ ps. Thus the isosbestic is moving toward the blue, asymptotically approaching λ_{1B}.

Figure 3b shows an expanded view of the near λ_{1B} data for HO. The data at 417.6 nm consists of a fast initial decay, and a slower decay, similar to that which is observed for PH at 416 nm. These data show that the dynamics of Fe--L species in PH and HO involve a fast (1–2 ps) and a slower (30–35 ps) process. The fast decay correlates with the appearance of Fe + L, while the slower decay correlates with the exponential part of the λ_{CO} decay. These observations furnish conclusive proof for the existence of *at least two* non-Fe–L or -Fe + L species present after photolysis of PH–CO and HO–CO.

As a control experiment, we monitored λ_{1B} decays in a 300 K PH–CO solution. At 300 K, process I* is absent, and all photolyzed Fe–L molecules relax into Fe + L with a time constant of 300 fs.[15] At λ_{1B} we observed only fast, instrument-limited decays. The ≈30-ps tail in the 100 K data associated with process I* had vanished.

The amplitudes of the transients observed near λ_{1B} furnish some information about the absorption spectra of the Fe--L species. Assuming for the moment that these species do not absorb in the region of interest, eq 3 and the spectral parameters of PH and

(24) Petrich, J. W.; Martin, J. L.; Houde, D.; Poyart, C.; Orszag, A. *Biochemistry* **1987**, *26*, 7914.

HO would predict the maximum ΔOD at λ_{1B} to be 0.7 for PH and 0.4 for HO. The observed values are 0.35 (PH) and 0.18 (HO), substantially less than the predicted values. This qualitative observation indicated that Fe--L produced by photolysis of Fe–L possesses a small absorbance at λ_{1B}, as eq 3 shows that absorption by Fe--L tends to reduce the ΔOD value. A quantitative analysis of this point is provided below.

We observe two very different rebinding processes and two very different decay processes for the Fe--L species. It is natural to assume that each rebinding process has a corresponding Fe--L. There are two distinct ways this behavior can occur, which we can term *inhomogeneous* hemes, or *homogeneous* hemes.[2,4] In the inhomogeneous case, the sample consists of two distinct types of environments, each giving rise to its distinctive rebinding kinetics. Interconversion between these environments is slow or negligible on the timescale of the inverse PRF. There will be no direct spectral evidence for the presence of two distinct Fe–L species if the frequency shift introduced by the differing environment is small compared to the large width, $\Delta\nu \approx 16$ nm, of the Fe–L Soret transition.[9] In the homogeneous case, each Fe–L molecule has two parallel channels for Fe--L formation and subsequent ligand rebinding, so every molecule is a potential candidate for creation of either Fe--L intermediate.

The homogeneous and inhomogeneous models can be distinguished via *multiple flash experiments*.[2,4] If we choose a PRF which is large relative to the rate[25] of process I but small relative to the rate of I*, after a few pulses, homogeneous hemes would repeatedly be offered the choice of entering the long-lived or short-lived states. They would eventually all be pumped into the long-lived process I states and the transient corresponding to process I* would vanish. Conversely, inhomogeneous hemes would not experience this pumping process, and at high PRF, process I* would not vanish. Chan[9] performed multiple flash experiments on PH–CO at 10 K using long (μs), high-energy (100 mJ) pulses at 540 nm, and observed only a small amount of pumping.

We also performed a multiple flash experiment in the following manner. Operating at a PRF of 130 Hz, we lowered the sample temperature to 15 K. At this temperature, we obtain the necessary conditions[25] to distinguish between the two models. Process I*, with its gentle temperature dependence,[6] will have a rate of $\approx 10^9$ s^{-1}, far faster than the PRF of 130 s^{-1}, while process I has slowed so that the (1/e) decay time exceeds 1 s.[5,9] We allowed the sample to equilibrate with the periodic optical pumping process for several seconds, and then scanned the variable delay line and averaged the results obtained over a few minutes. Under these conditions, homogeneous hemes would be almost totally pumped into the long-lived process I states.

Figure 4 gives the results of one multiple pulse run, comparing λ_{CO} data taken on PH–CO at 15 and 100 K. The prominent process I* decay seen at 100 K does not decrease appreciably in amplitude at 15 K, although the rate does decrease as expected. This experiment demonstrates that the short-lived process I* states are not pumped to any significant extent into the long-lived process I states. We have thus shown conclusively that interconversion between the two Fe–L species is at best difficult, so that the inhomogeneous limit is approached or met in the PH system. The small amount of pumping observed by Chan using long, intense laser pulses, does suggest that interconversion can occur by laser-induced local heating.

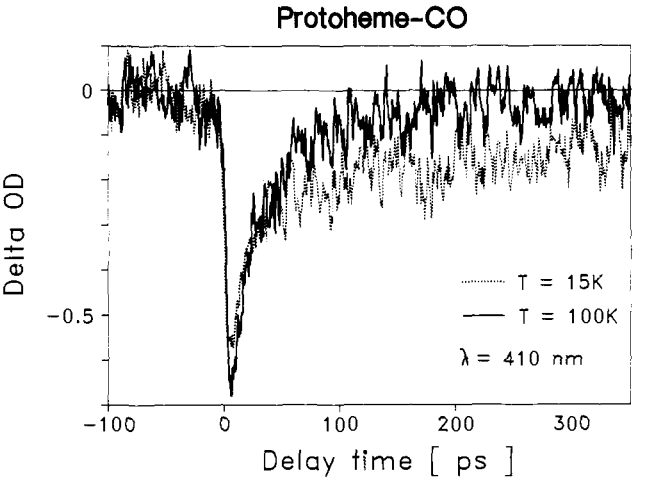

Figure 4. Results of a multiple flash experiment on PH–CO at λ_{CO} = 410 nm. At 100 K, both process I and I* are fast relative to the laser pulse repetition frequency (PRF) of 130 s^{-1}. At 15 K, process I* is fast relative to the PRF, while process I is far slower than the PRF. Under these conditions, homogeneous hemes would all be pumped into the long-lived process I states, and the large amplitude transient corresponding to process I* would vanish. This pumping does not occur, demonstrating that the subensembles responsible for process I and I* are *independent* and *inhomogeneous*.

Discussion

Kinetic Model. A successful model of the wavelength-dependent kinetics must account for the following observations.

1. Ligand rebinding consists of *two processes*, a ≈30-ps exponential process, process I*, and a slower, nonexponential process, process I.

2. The quantum yield for formation of Fe + L from Fe–L, f, is <1.

3. The appearance of Fe + L is delayed by a few picoseconds relative to the disappearance of Fe–L.

4. The isosbestic is time dependent for $\tau < 150$ ps, and kinetic decay data near λ_{1B} always show a fast and slow component, indicating the presence of *at least two* intermediate species, one whose decay matches the rise time of Fe + L, and the other whose decay matches process I*.

5. The heme sample consists of two distinct subensembles, one associated with process I and the other associated with process I*. These subensembles are not interconverted by optical pumping.

These observations definitively rule out the relatively simple kinetic model where photolysis of Fe–L produces a single Fe--L species which can either go on to form Fe + L and rebind via process I, or rebind CO via process I*. We must therefore look to a more complicated model, and thus propose the following.

Two distinct types of Fe–L species have been shown to be present in the frozen glass environment. One type, which we denote Fe^{I}–L is associated with the faster intermediate, which we denote Fe^{I}--L. The Fe^{I}--L species relaxes within a few picoseconds into the Fe + L species. Because this relaxation process involves heme "doming" along with associated electronic state and spin changes, we denote the rate constant for relaxation $k_D(T)$. Once Fe + L is produced, it rebinds via process I to re-form Fe^{I}–L. Process I is not described by a rate constant, as it is nonexponential. Rather it is described by a rate function $k_I(t,T)$, which obeys the Arrhenius relation for a system with distributed barriers. Alberding et al.[5] have shown that the time-dependent "survival fraction", $N(t,T)$, of Fe + L species is given by the algebraic power law function

$$N(t,T) = [1 + t/t_0(T)]^{-n(T)} \quad (4)$$

where t_0 and n are temperature-dependent parameters which completely specify the kinetic decay function. Thus $\int dt\, k_I(t,T) \propto [1 + t/t_0(T)]^{-n(T)}$.

The other type of Fe–L species, which we denote Fe*–L is associated with the slowly decaying Fe*--L species and process I*. The Fe*--L rebinds directly with a ligand to produce Fe*–L with rate constant $k^*(T)$.

We denote the equilibrium fraction of Fe^{I}–L as f; i.e., f is the fraction of hemes which will relax with rate constant k_D and then rebind via process I. Alternatively, f is the quantum yield for production of Fe + L from all Fe–L species. Similarly, $1 - f$ is the fraction of Fe–L which will, if photolyzed, rebind via process I*. With this notation, our proposed kinetic model for PH and HO at a particular low temperature, where ligand rebinding via

(25) Strictly speaking, process I has no "rate", as it is nonexponential, and thus an endless process. Operationally we can find a PRF which is fast relative to the half-life of process I, which is then slow relative to the rate of process I*.

solvent processes can be neglected, is

$$Fe^{1}\text{–}L \xrightarrow{h\nu} Fe^{1}\text{--}L \quad (5)$$

$$Fe^{1}\text{--}L \xrightarrow{k_D} Fe + L \quad (6)$$

$$Fe + L \xrightarrow{k_1(t)} Fe^{1}\text{–}L \quad (7)$$

and

$$Fe^{*}\text{–}L \xrightarrow{h\nu} Fe^{*}\text{--}L \quad (8)$$

$$Fe^{*}\text{--}L \xrightarrow{k^{*}} Fe^{*}\text{–}L \quad (9)$$

We can then write the appropriate differential equations for eq 5–9. We find that analytic solutions can be obtained for each species given the initial condition of efficient, impulsive photolysis. These solutions are

$$[Fe^{1}\text{--}L](t) = fN^{0} \exp(-k_D t) \quad (10)$$

$$[Fe^{*}\text{--}L](t) = (1 - f)N^{0} \exp(-k^{*}t) \quad (11)$$

$$[Fe + L](t) = fN^{0}(k_D t_0)^{-n} \exp(k_D t_0)(1 + t/t_0)^{-n}\, \gamma(n + 1, k_D t) \quad (12)$$

and

$$[Fe^{1}\text{–}L](t) + [Fe^{*}\text{–}L](t) = N^{0} - [Fe^{1}\text{--}L](t) - [Fe^{*}\text{--}L](t) - [Fe + L](t) \quad (13)$$

where $\gamma(\alpha,\beta)$ is the incomplete gamma function,[26] which occurs because of the algebraic power law form of process I, and N^0 is the initial concentration of carboxy hemes. We do not distinguish between Fe^1–L and Fe^*–L in our experiments, as their absorption spectra are unresolved.

The observable in our experiments is $\Delta OD_\lambda(\tau)*I(\tau)$, the delay time-dependent change in OD at wavelength λ convolved[20] with the laser instrument response $I(\tau)$. In turn, ΔOD is related to the number densities, $[Fe + L](t)$, etc., through a set of extinction coefficients which can be determined independently for the stable carboxy and deoxy species but which cannot be readily determined for the short-lived intermediates. The finite duration instrument response is important only in the analysis of the short time ($\tau <$ 5 ps) data. If a molecular response is imagined to be a step or delta function, the apparatus will round off the sharp corners. For example, if the molecular response is a delta function with $\Delta OD_{max} = 1.0$, the observed decay will follow the apparatus response, and its maximum value will be somewhat smaller than unity. The round-off effect should be considered in the quantitative computation of the quantum yield for Fe + L production and the absorbance of Fe--L at λ_{IB}, quantities which are determined by the relative amplitudes of our decay curves near $\tau = 0$.

The procedure we used was to fit the λ_{CO} and λ_{DL} data using the known extinction coefficient ratios by varying the values of five parameters: k_D, k^*, n, t_0, and f in eq 8–11. Fortunately, the interdependence of these parameters is not great. First we determine k_D by fitting the short time behavior of the λ_{CO} and λ_{DL} data shown in Figure 2. Then we determine the value f by fitting the quantum yield for production of Fe + L from Fe–L as discussed in the Results. The values of n and t_0 are determined by the nonexponential process I, which dominates the λ_{CO} and λ_{DL} decays at long time ($\tau >$ 150 ps). Finally the process I decay is subtracted away from the λ_{CO} data, and the resultant process I* decay can be fit with k^*. Having determined a preliminary fit, we further tested these parameters by comparison with data taken at a variety of wavelengths between 395 and 440 nm until good consistency was obtained. The values we obtained at 100 K for PH and HO are given in Table I. The calculated curves for λ_{CO} and λ_{DL} are shown in Figure 1. These calculations are clearly an excellent fit to the data at all times.

We then examined the isosbestic data in Figure 3 in light of this fitting procedure. We were able to readily reproduce the functional forms of these decays using the parameters in Table I, but our calculated quantum yields (amplitudes) were always too large, as discussed in the Results. This difficulty can be removed if we suppose that the Fe--L species possess a broad, weak absorption near λ_{IB}. This supposition was suggested by previous work of Caldwell et al.[13] on photodissociation of synthetic heme complexes similar to those studied in this work. They observed photointermediates in the same wavelength ranges as the Fe–L species, but with somewhat smaller absorbance. For the example of PH, we observe a ΔOD maximum at λ_{IB} of 0.35, while the absorption spectrum predicted 0.7, assuming that Fe--L did not absorb at λ_{IB}. However, this does not imply that the Fe--L absorbance is $\approx$50% of the Fe–L or Fe + L absorbance at λ_{IB}, because of the round-off effect of finite pulse duration. Instead, we find that if Fe--L absorbance is about 15% of Fe–L or Fe + L absorbance at λ_{IB}, we accurately fit *all* the data near λ_{IB}, for example, that shown in Figure 1.

Table I. Comparison of Kinetic Parameters of Protoheme–CO (PH) and Heme Octapeptide–CO (HO) in Glycerol–Water (75:25) at 100 K

parameter	protoheme	heme octapeptide
$1/k_D$,[a] ps	1.5 ± 0.3	1.0 ± 0.3
$1/k^*$,[b] ps	30 ± 5	35 ± 5
f[c]	0.7 ± 0.1	0.8 ± 0.1
t_0,[d] ps	15 ± 3	6 ± 2
n[d]	0.98 ± 0.05	0.25 ± 0.05

[a] The parameter k_D, defined in eq 6, is the T = 100 K rate constant for heme relaxation, or "doming". [b] The parameter k^*, defined in eq 9, is the rate constant for process I* at T = 100 K. [c] The parameter f, defined in eq 10 and 11, is the quantum yield for production of Fe + L from all Fe–L species present. [d] The parameters t_0 and n are defined in eq 4, and they characterize the algebraic power law decay of process I.

Because the important species involved in the photolysis process all have spectra which overlap to some extent, the kinetic data in Figures 1 and 2 do not present a completely accurate picture of the time-dependent populations. Rather each species contributes to an extent determined by the relative extinction coefficients. For example, the decay at λ_{CO} has a contribution from the absorption of Fe + L as well as Fe–L. When Fe^1–L is photolyzed, its absorption vanishes, creating some Fe--L, which is only weakly absorbing. The Fe^1--L decays to form Fe + L, whose absorption at λ_{CO} causes the λ_{CO} decay to have a fast component which decays with rate constant k_D, and which thus has no relationship to the Fe + L dynamics. As shown in eq 2, at λ_{IB} the contributions from Fe + L and Fe–L cancel, and the decay consists solely of the Fe--L species dynamics.

Using our experimental kinetic data, we can directly calculate the normalized time-dependent populations of each species in PH and HO at 100 K, assuming impulsive excitation. The population plots are shown in Figure 5. The Fe–L population is the sum of the Fe^1–L and Fe^*–L populations. The populations are normalized so that $\Sigma p_i(t) = 1$, where $p_i(t)$ is the population of the ith specie.

Physical Picture. At 298 K, in a nonviscous fluid medium, Fe–L is present as a single species, and photolysis produces an Fe--L intermediate which relaxes to form Fe + L on the subpicosecond timescale.[15,24] The relaxation process results in a "doming" of the initially planar heme. When the glass is frozen, photolysis results in two parallel, independent channels. We thus proposed the existence of two liganded species, Fe^1–L and Fe^*–L. These species are chemically identical, but differ in the local structure of their glass cages. The spectral perturbation induced by the solvent cage is not large compared to the intrinsic width of the absorption spectra. As T is decreased, more molecules populate the Fe^*–L state, and the fraction of Fe^*–L increases relative to Fe^1–L; at T = 100 K, 20–30% of the hemes present are in the Fe^*–L state. Interconversion between these two states is slow or absent at 100 K.

Photolysis of Fe^1–L creates the Fe^1--L intermediate which relaxes within a few picoseconds to a species whose absorption maximum, within the precision of our measurements, is identical

(26) Abramowitz, M., Stegun, I. A., Eds. *Handbook of Mathematical Functions*; Dover: New York, 1972; Chapter 6.

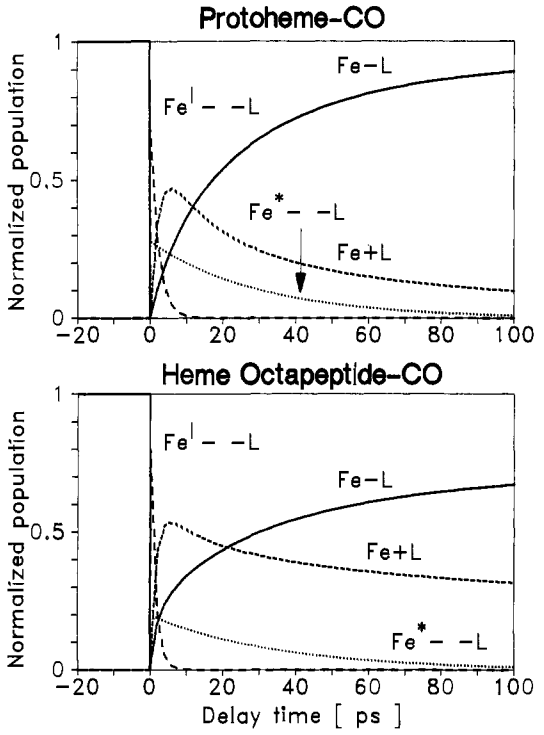

Figure 5. Time dependent populations of the Fe–L species (solid curve), Fe--L intermediate (large dashes), Fe*--L intermediate (dotted line), and Fe + L species (small dashes), deduced from the fitting procedure of the kinetic multispectral data.

with that of the stable, relaxed Fe + L. Thus we identify this relaxation with the doming process. The relaxed Fe + L rebinds via thermally activated, nonexponential process I. Photolysis of Fe*–L creates the Fe*--L intermediate which does not relax into Fe + L, but rather rebinds via exponential process I*, a process which does not involve surmounting a classical, enthalpic barrier.

Heme Relaxation. Martin et al.[15] studied PH relaxation after excitation of PH–CO with 307-nm, 300-fs pulses at room temperature in a polyethylene glycol–water solution which is less viscous than our glycerol–water glass. They observed the formation of a λ_{max} = 425 nm deoxy heme occurring in 350 fs, compared with our 100 K value of 1.5 ps. Unfortunately, a direct comparison of our results is not possible at this time because the experiments differ in three crucial areas: viscosity, temperature, and excitation wavelength. Martin et al. also observed a 3.2-ps decay at 410 nm which was attributed to excited liganded species which relax to the ground state with this time constant. This second relaxation process is possibly an artifact of 307-nm excitation. Unlike our experiments, where hemes are excited at the ^{1}Q origin at 570 nm, 307-nm excitation produces more than 15 000 cm^{-1} of excess heat for each absorbed photon. The interpretation of the 3.2-ps decay as heme cooling is further supported by the recent Raman studies of Petrich et al.[24]

We also observe the dynamics of the Fe*–L intermediate in PH and HO. The Fe*–L does not relax to form Fe + L. The cause of this hindered relaxation is undoubtably the frozen glass matrix, since process I* is not significant at high temperatures.[6] The non-Arrhenius behavior of process I* strongly suggests that Fe*--L remains planar even when deligated, as an investiment of energy would be required for a nonplanar heme to attain a planar transition state. We associate the hindered relaxation of Fe*–L with tight, highly connected cages. The volume of each glass cage is certainly not identical, rather it must be characterized by a distribution function. Glycerol water mixtures can form extensive hydrogen-bonding networks, suggesting that individual cages may also differ significantly in their connectivity, or in their interactions with chemical substituents on the periphery of the porphyrin.

Process I. Process I in PH and HO has been studied by Frauenfelder's group[5,9] over a wide range of temperature, but with insufficient time resolution ($t_r \approx 1$ μs) to observe the dynamics we report. Instead, their direct observations of process I were restricted to $T \leq 80$ K, where rebinding was slow enough to be observed. They determined the value of the exponents $n(T)$ in eq 2 over this temperature range, but could not determine the value of $t_0(T)$ at any temperature. We now know that t_0 is on the order of 10^{-11} s. Alberding et al.[5] plot the observed values of $n(T)$ versus T for PH. By extrapolation to 100 K, they predict a value of $n \approx 1$, in excellent agreement with our result.[5,9] It is clear, both from this analysis and from our earlier temperature-dependent work,[6] that the nonexponential ligand rebinding in PH is the same process I observed by Frauenfelder.[5]

The nonexponential kinetics of process I were attributed to a distributed enthalpic and entropic barrier which is an intrinsic property of the heme and its solvent glass.[5] In other words, the hemes exist in a number of conformational substates[1,2,4,5] which are similar in overall form and function, but which differ in details. Nonexponential recombination implies that the process of interconversion between these substates, namely conformational relaxation, is slow relative to the barrier crossing. When conformational relaxation is fast relative to barrier crossing, each ligand sees the same time-averaged barrier, and rebinding is exponential. For example, in isolated β chains of hemoglobin at 300 K,[27] process I is exponential with τ = 1 ns, indicating that conformational relaxation of the protein and solvent occurs faster than 10^9 s^{-1}. For PH at 300 K, process I is nonexponential,[6] and the relevant time scale of conformational relaxation is roughly 50 ps, the half-life of process I. Significantly, the NMR correlation time of glycerol at 300 K is about 100 ps,[28] and we conclude that motional averaging of the solvent cage surrounding heme is slower than ligand rebinding at all temperatures up to 300 K.

Process I*. The quantum efficiency for heme relaxation followed by process I rebinding is on the order of 0.7. Hill et al.[6] found that f = 0.2 at 100 K for PH, but their value was erroneous, as it was based on kinetic data obtained at a single value of λ = 565 nm, rather than a detailed multispectral analysis. The hemes which do not relax do repopulate the PH–CO or HO–CO state (determined by absorption recovery at λ_{CO}) in τ = 30 ps (PH) and τ = 35 ps (HO). We interpret process I* as arising from ligand rebinding to heme which has not relaxed. The hindered relaxation may be a consequence of a glass cage which is too constricted to permit the doming process to occur. In this case, the exponential time dependence of process I* is reasonable, because with Fe in the plane and CO close by, there may be very few conformational substates available.[17]

We have considered an alternative mechanism, namely that a subensemble of the Fe–CO species do not dissociate, but rather populates a liganded electronic excited state which has little absorption in the 400–440-nm range, and which relaxes nonradiatively back to the liganded ground state on the 30-ps time scale. Excited states of Fe porphyrins generally decay on the subpicosecond time scale.[29] One notable exception is the porphyrin $\pi \rightarrow \pi^*$ triplet of iron(III) tetraphenylporphyrin chloride, which has a 30-ps lifetime.[11] However, triplet-state buildup can be ruled out as the cause of the process I* transient. In Fe porphyrins, most molecules return to the ground state on a time scale shorter than our 2-ps laser pulse,[11,29] while only a small fraction populate the triplet state by intersystem crossing.[11] Under these circumstances, the triplet population will increase with the intensity of the photolysis pulse, via multiple rephotolysis. However, we observe that the *relative* amplitudes of processes I and I* are

(27) Dlott, D. D.; Frauenfelder, H.; Langer, P.; Roder, H.; DiIorio, E. E. *Proc. Natl. Acad. Sci. U.S.A.* **1983**, *80*, 6239. Ansari, A.; DiIorio, E. E.; Dlott, D. D.; Frauenfelder, H.; Iben, I. E. T.; Langer, P.; Roder, H.; Sauke, T. B.; Shyamsunder, E. *Biochemistry* **1986**, *25*, 3139.

(28) Koivula, E.; Punkkinen, M.; Tanttila, W. H.; Ylinen, E. E. *Phys. Rev.* **1985**, *B32*, 4556.

(29) Adar, F.; Gouterman, M.; Aronowitz, S. *J. Phys. Chem.* **1980**, *80*, 2184. Andrews, J. R.; Hochstrasser, R. M. *Proc. Natl. Acad. Sci. U.S.A.* **1980**, *77*, 3110. Champion, P. M.; Albrecht, A. C. *J. Chem. Phys.* **1979**, *71*, 1110; **1980**, *72*, 6498. Champion, P. M.; Lange, R. *J. Chem. Phys.* **1980**, *73*, 5953. Bersohn, R. B. *Jerusalem Symp. Quantum Chem. Biochem.* **1982**, *15* (Intramol. Dyn.), 497.

independent of the photolysis pulse intensity. Other difficulties with this proposed mechanism are that experiments performed on PH with no bound sixth ligand show no evidence for excited states with appreciable ($\tau > 1$ ps) lifetimes, and that the rate of process I* is a roughly linear function of T, behavior which is not normally associated with internal conversion or intersystem crossing relaxation processes.[30]

Process I* does not obey the Arrhenius relation, and the observed linear dependence on temperature indicates the absence of a sizable enthalpic barrier to rebinding. The simplest description of chemical reactions is transition-state theory (TST)[31] which gives the rate constant as

$$k^* = (k_B T/h) \exp(\Delta S^+/k_B) \exp(-\Delta H^+/k_B T) \quad (14)$$

where the + indicates activation entropy or enthalpy. At 100 K, $k^* = 3.3 \times 10^{10}$, and $(k_B T/h) = 2 \times 10^{12}$. Thus the exponential factors in eq 14 contribute $\approx 1.7 \times 10^{-2}$. The activation entropy describes the reduction in degrees of freedom occurring in the transition from bound to free ligand, and contains contributions from the loss of rotational and translational freedoms as well as possible spin changes at Fe.[32] Equation 14 is satisfied for $\Delta S^+/k_B \approx -4$. The loss of rotational entropy[32-34] accounts for $\approx 5k_B$ of entropy loss, showing that process I* involves almost no translational entropy loss. By contrast, for process I rebinding in myoglobin (Mb), where the ligand inhabits a pocket of volume $V \approx 30$ Å^3, the translational entropy loss is $8k_B$.[32] Our analysis shows that process I* involves almost no translational motion of CO, merely a simple rotation. In this respect, process I* resembles low-temperature tunnel rebinding of CO to myoglobin,[4] where the importance of rotations was demonstrated via anomalous isotope effects on the tunneling process.[35] Jongeward et al.[36] have characterized a similar ultrafast rebinding process to Mb as involving a "contact pair" consisting of the heme and ligand. Although we possess no direct structural information indicating that Fe and CO are in contact, the absence of translational entropy suggests that this description is apt for process I*.

The extremely large rate of process I* also suggests that friction or nonadiabatic barrier crossings[32,37] play a minimal role. It is still controversial as to whether process I, which requires a transition from $S = 2$ to $S = 0$, involves nonadiabatic barrier crossings.[32] The spin transition for process I involves a second-order spin–orbit coupling matrix element whose small magnitude is surmised to have an appreciable effect on process I.[37] Although we have no direct experimental evidence for the spin state of the Fe--L intermediates, in the event that they possess a spin $S < 2$, the spin–orbit interaction should be large enough to render the rebinding process adiabatic.

Conclusion

We have examined the ultrafast multispectral decay kinetics of PH–CO and HO–CO in glycerol–water glass at 100 K. Our experiments indicate that the chemical kinetics proceed as if there were two independent subensembles of reactants, which we term Fe^1–L and Fe*–L. Photolysis of Fe^1–L [$\lambda_{CO} = 410$ (PH) and $\lambda_{CO} = 415$ nm (HO)] produces, with a delay time of a few picoseconds and a quantum yield of 0.7 (PH) or 0.8 (HO), a new species with the same absorption maximum, $\lambda_{DL} = 423$ nm (PH) or 425 nm (HO), as the equilibrium deoxy Fe + L species. We cannot yet determine with accuracy whether the spectrum of this species is identical with that of the relaxed deoxy heme, but it is certainly quite similar. At the isosbestic point, where contributions from deoxy and carboxy hemes cancel, we observe two distinct transient intermediates with weaker absorbance. The decay of the fast transient [$\tau = 1.5$ ps (PH) and $\tau = 1.0$ ps (HO)] is exactly correlated with the appearance of the relaxed, deligated heme. This transient Fe--L species is probably an unrelaxed five-coordinate heme which absorbs only weakly (ca. 15% of the absorption of Fe–CO) in this region, and we associate the relaxation process with nonradiative electronic processes, probable spin changes, and vibrational relaxation, or "doming". This doming process is faster in HO compared to PH, as a consequence of the basket handle peptide. This effect of the peptide may be caused by proximal tension, or by screening the proximal face of the porphyrin from the solvent.

Once the relaxed heme is created, it rebinds by process I, an Arrhenius process characterized by a distributed barrier. Process I is considerably slower in HO than in PH at 100 K, a manifestation of the well-known proximal tension effect of basket handle hemes, which require a greater investment of energy to attain the planar transition state than do bare hemes.

The remaining Fe*–L hemes do not relax after photolysis, probably because they are hindered by their constricting glass cages. This conclusion is supported by the slightly larger quantum yield for relaxation of HO relative to PH, inasmuch as HO is protected from the solvent on the proximal side. Also the negligible translational entropy change for process I* rebinding shows that CO does not occupy a significantly larger free volume when dissociated. Ligand rebinding to unrelaxed, planar heme, process I*, has nearly the same rate in PH and HO. Again, this is consistent with our interpretation of rebinding to planar heme, as the proximal peptide chain should have negligible effect on a ligand approaching a planar heme from the distal side. The absence of a sizable enthalpic barrier to rebinding also implies that the heme is planar. The only physical processes which limit the rate of process I* are the finite collision frequency along the reaction coordinate, $k_B T/h$, and the rotational entropy loss of $\Delta S^+_{rot} \approx 5k_B$.

It is interesting that our PH and HO kinetics can be fit with a model involving two intermediates and two rebinding processes, rather than a distributed intermediate and many rebinding processes. Grenoble et al.,[38] who used absorption and Mössbauer spectroscopy, found that the ground state of 298 K deligated PH, which is domed, with high-spin ($S = 2$) Fe is converted to an intermediate or mixed spin state with the application of high pressure. Thus the activation volume for heme doming is positive, and it is reasonable to suppose the coexistence of tight glass cages which inhibit doming, for which intermediate spin Fe + L states are stable, along with looser cages which do not inhibit doming, for which high-spin Fe + L states are stable.

Acknowledgment. This research was supported by the National Science Foundation, Division of Materials Research, through Grant NSF DMF 87-21243. D.D.D. thanks Professor M. D. Fayer for gracious hospitality during his sabbatical stay at Stanford University.

(30) McGlynn, S. P.; Azumi, T.; Kinoshita, M. *Molecular Spectroscopy of the Triplet State*; Prentice Hall: Englewood, NJ, 1969.
(31) Glasstone, S.; Laidler, K. J.; Eyring, H. *The Theory of Rate Processes*; McGraw-Hill: New York, 1941.
(32) Frauenfelder, H.; Wolynes, P. G. *Science* **1985**, *229*, 337.
(33) Moelwyn-Hughes, E. A. *Physical Chemistry*; Pergamon Press: Oxford, 1961; pp 431–435.
(34) Collman, J. P.; Brauman, J. I.; Suslick, K. S. *J. Am. Chem. Soc.* **1975**, *97*, 7185.
(35) Alben, J. O.; Beece, D.; Bowne, S. F.; Eisenstein, L.; Frauenfelder, H.; Good, D.; Marden, M. C.; Moh, P. P.; Reinisch, L.; Reynolds, A. H.; Yue, K. T. *Phys. Rev. Lett.* **1980**, *44*, 1157.
(36) Jongeward, K. A.; Magde, D.; Taube, D. J.; Marsters, J. C.; Traylor, T. G.; Sharma, V. S. *J. Am. Chem. Soc.* **1988**, *110*, 380.
(37) Gerstman, B.; Austin, R. H.; Hopfield, J. J. *Phys. Rev. Lett.* **1981**, *47*, 1636. Austin, R. H.; Chang, A. M. F.; Gerstman, B. S.; Rokhsar, D. *Comments Mol. Cell Biophys.* **1985**, *2*, 295.
(38) Grenoble, D. C.; Frank, C. W.; Bargeron, C. B.; Drickamer, H. G. *J. Chem. Phys.* **1971**, *55*, 1633.